A Comparison of Convective and Non-Convective Cirrus Cloud Microphysics

M. R. Poellot and R. J. Zerr
University of North Dakota
Grand Forks, North Dakota

Introduction

It is likely that the microphysical characteristics of convective and non-convective cirrus clouds are significantly different, given the dissimilar nature of their origins. Thunderstorm anvils are produced through the rapid lifting of boundary-layer air, while jet stream and other cirrus (excluding aircraft contrails) are formed by relatively weak vertical motions in upper tropospheric air. It is also possible that the anvil cirrus properties may change with age as the cloud drifts away from its source. These microphysical differences must be considered in order to successfully model their radiative impact.

Two anvil clouds (one fresh, one old) were sampled by the University of North Dakota Citation aircraft during the 1994 Remote Cloud Sensing Intensive Observation Period (IOP), along with non-convective cirrus. Satellite images (Figures 1 through 4) show the old anvil cloud, no longer associated with active convection (orphaned), originated

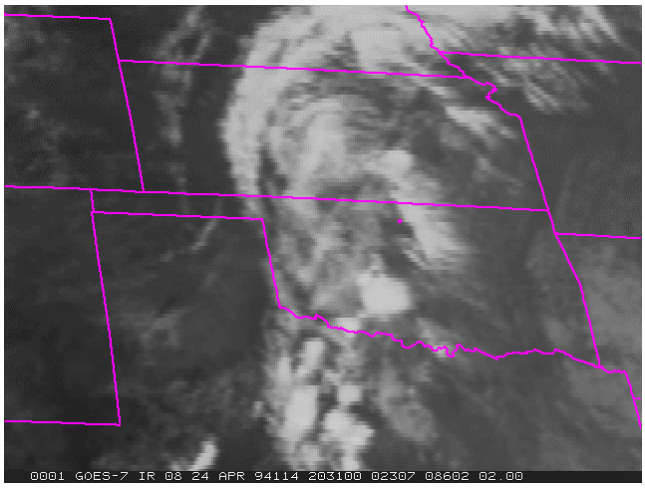

Figure 1. Geostationary Operational Environmental Satellite (GOES) infrared (IR) image of orphan anvil at 2031 UTC, 24 April, 1994. The ARM SGP site is indicated by a dot in north-central Oklahoma.

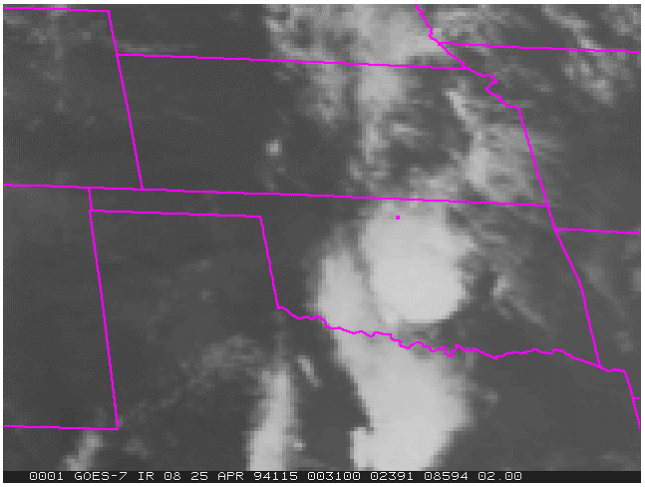

Figure 2. GOES IR image of fresh anvil at the time of the first profile, 0031 UTC, 25 April, 1994.

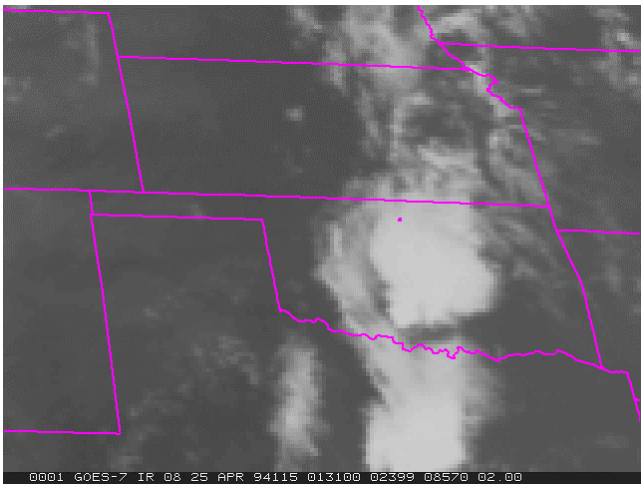

Figure 3. GOES IR image of fresh anvil at the end of the first descent profile, 0131 UTC, 25 April, 1997.

over southwest Oklahoma 6 to 8 hours before sampling on 24 April. The anvil sampled 4 to 7 hours later on 25 April was being produced by vigorous convection near the Atmospheric Radiation Measurement (ARM) Southern

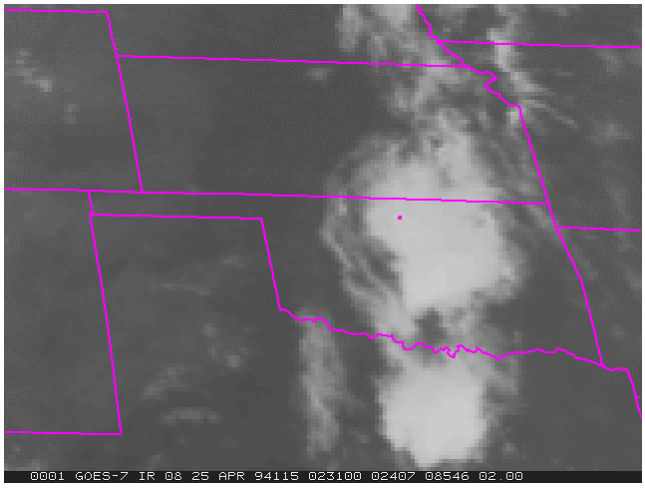

Figure 4. GOES IR image of fresh anvil at end of sampling, 0231 UTC, 25 April, 1994.

Great Plains (SGP) site. One spiral ascent was made through the orphan anvil and a series of two spiral ascents and descents were accomplished through the fresh cloud. Cloud top was never reached in the latter case due to air traffic control constraints. During the sampling of the fresh anvil, the active sensors located at the Central Facility (lidars and mm-wavelength radars) were unable to penetrate the full depth of the cloud due to signal attenuation.

Vertical profiles of the anvil microphysics are presented in Figures 5 through 8. The two-dimensional cloud (2DC) probe on the Citation has an effective minimum imaging size threshold of 66 μm. Concentrations of these larger particles (not shown) had a peak value of less than 200/L. The 2DC shadow, or data, include zero-area images and here indicate the presence of regions of smaller particles in concentrations of hundreds per liter. The 2DC mean diameters are calculated for only the larger particles (>66 μm). Condensation nuclei concentrations are also plotted to show the presence of boundary-layer air that has been transported to the upper troposphere.

The old anvil is seen to contain high concentrations of small ice crystals in the upper portion of the cloud, with generally fewer but larger particles in the lower two-thirds of the cloud. There is also a greater degree of scatter in the mean sizes of the larger particles. The fresh anvil also had smaller crystals in the upper portion with increasing diameters toward the base. The values of mean diameter were more uniform in the new cloud. Pockets of particle concentrations in excess of 500 L were noted between 9.7 km and 10.2 km mean sea level.

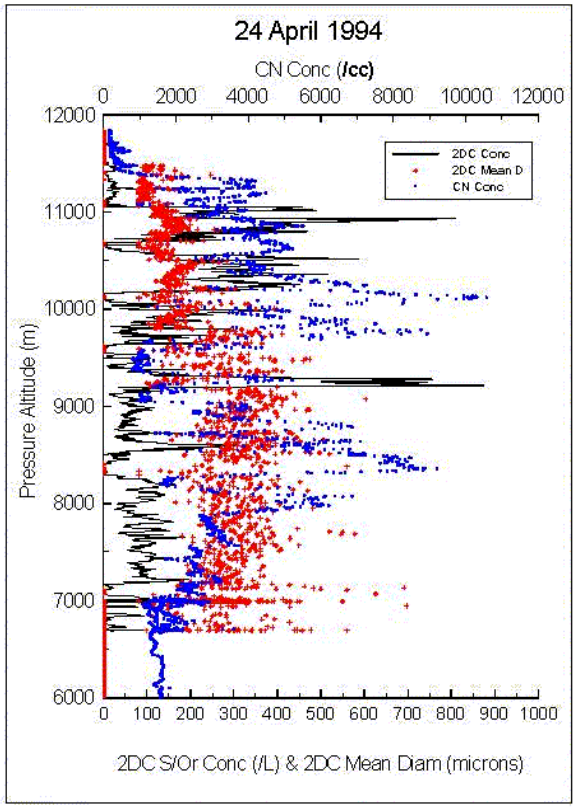

Figure 5. Vertical profile of orphan anvil, 24 April, 1994. (For a color version of this figure, please see *http://www.arm.gov/docs/documents/technical/conf_9803/poellot-98.pdf)*.

Particle size distributions for the top, middle, and lower portions of both anvils are shown in Figures 9 through 11. The spectra are seen to broaden as you move from the top to the bottom of the cloud where there are larger particles. This is likely due to sedimentation and aggregation processes. It should also be noted that the size distributions of the fresh anvil have a bimodal character in the middle and lower cloud regions, with a secondary peak around 200 μm to 300 μm. This is less pronounced in the orphan anvil.

Also presented on the spectral graphs are the average size distributions for non-convective cirrus clouds sampled during the First International Satellite Cloud Climatology Program (ISCCP) Regional Experiment (FIRE) Cirrus intensive field observation (IFO) II over Kansas in 1991. While the numbers of smaller ice crystals are comparable for the two cloud types, the number of particles larger than 150 μm found in the non-convective cirrus are 1 to 2 orders of magnitude less than in the anvils. The non-convective cirrus particles also had a bimodal distribution, with a secondary peak near 150 μm.

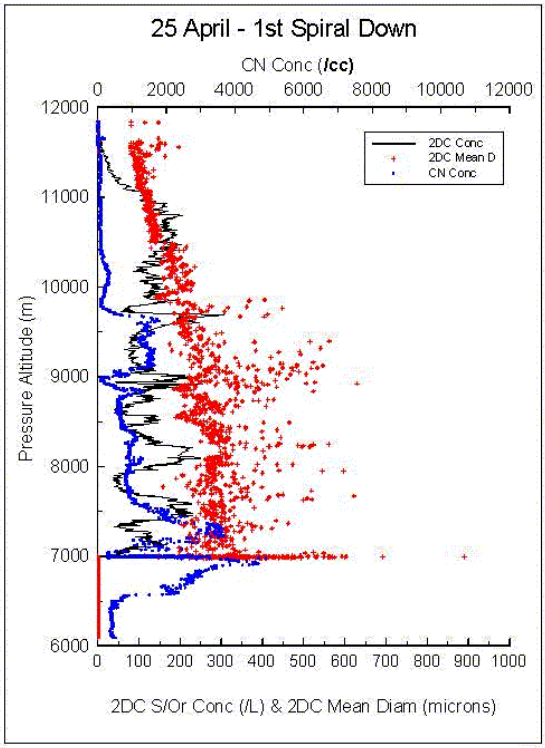

Figure 6. Vertical profile of fresh anvil, first descent spiral, 25 April, 1994. (For a color version of this figure, please see *http://www.arm.gov/docs/documents/technical/conf_9803/poellot-98.pdf*).

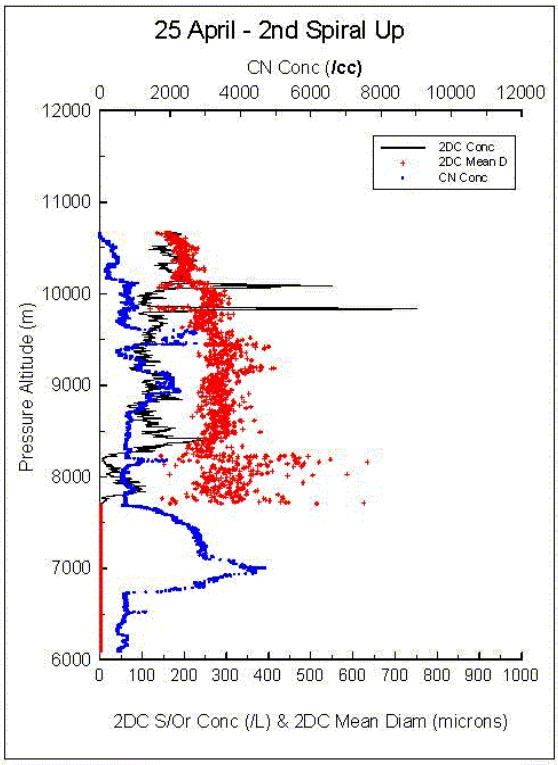

Figure 7. Vertical profile of fresh anvil, drums ascent spiral, 25 April, 1994. (For a color version of this figure, please see *http://www.arm.gov/docs/documents/technical/conf_9803/poellot-98.pdf*).

The data presented here strongly suggest that different microphysical parameterizations are required to accurately model the radiative transfer through convective and non-convective cirrus clouds. The anvil clouds studied here contained many more large particles and were optically thick. Further analysis is being conducted to examine the role of ice crystals smaller than the detection limit of the 2DC. Replicator data collected during these flights will be analyzed to determine the contribution of particles down to 5 μm in diameter.

Acknowledgment

This research was supported by U.S. Department of Energy Grant No. DE-FG03-97ER62360.

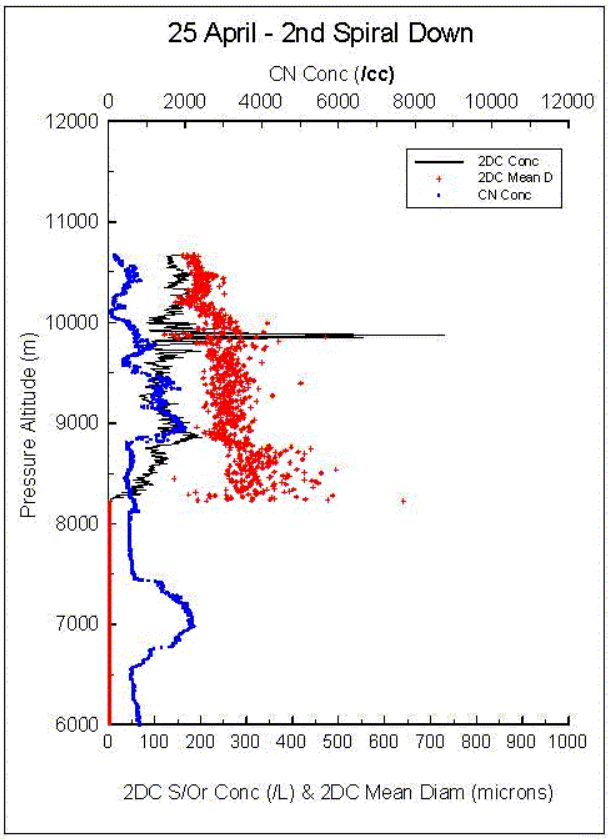

Figure 8. Vertical profile of fresh anvil, second descent spiral, 25 April, 1994. (For a color version of this figure, please see *http://www.arm.gov/docs/documents/technical/conf_9803/poellot-98.pdf*).

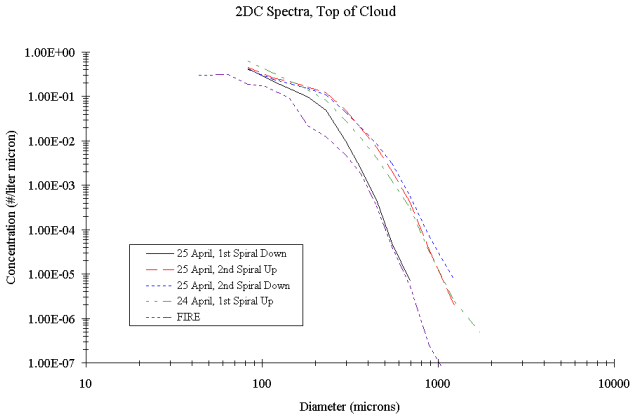

Figure 9. Particle size distributions in convective and non-convective (FIRE) cirrus, near cloud top. (For a color version of this figure, please see *http://www.arm.gov/docs/documents/technical/conf_9803/poellot-98.pdf*).

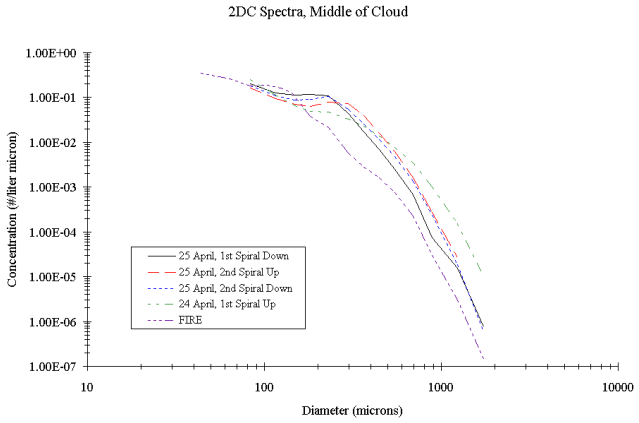

Figure 10. Particle size distributions in convective and non-convective (FIRE) cirrus, for middle of cloud. (For a color version of this figure, please see *http://www.arm.gov/docs/documents/technical/conf_9803/poellot-98.pdf*).

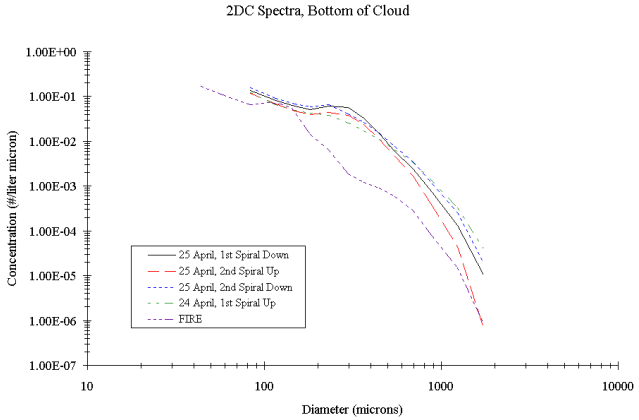

Figure 11. Particle size distributions in convective and non-convective (FIRE) cirrus, for bottom of cloud. (For a color version of this figure, please see *http://www.arm.gov/docs/documents/technical/conf_9803/poellot-98.pdf*).